DALTON
PERSPECTIVE

2-D NMR Spectroscopy of chiral phosphine complexes. Applications to problems related to enantioselective homogeneous catalysis

Paul S. Pregosin * and Gerald Trabesinger

Inorganic Chemistry ETH Zürich, Universitätstr. 6, CH-8092 Zürich, Switzerland

A 2-D NMR approach to elucidating problems of structure and dynamics in chiral organometallic phosphine complexes has been suggested. The examples chosen concern geometric isomers and prochiral face selection in allyl derivatives, a new bonding mode for atropisomeric chelates, chelate ring inversion, phenyl stacking, detecting small quantities of exchanging species and recognising equilibrating diastereomers. The methodology, which is based on X, ^{1}H correlation and NOE spectroscopy, is shown to be both versatile and potent.

1 Introduction

Nuclear magnetic resonance spectroscopy has become almost indispensable to the practising preparative organic chemist. It is one of the fastest ways to screen reactions and, at the same time, provides insights into molecular structure and solution dynamics. At a more sophisticated level, the analysis of subtle 2- and 3-D measurements (based on an ever-increasing number of pulse sequences[1]) has resulted in the solution of hundreds of complicated organic and biological structures, many of which concern small proteins.[2]

Historically, inorganic co-ordination chemists still rely heavily on X-ray crystallography. This community tends to shy away from 'sporting methods' and to some extent, this tradition has been carried forward into organometallic chemistry. Homogeneous catalysis, and particularly enantioselective catalysis, combines fundamental aspects of inorganic transition-metal chemistry with the mature elegance of organic carbon architecture.[3] The former discipline provides the template for bringing the correct pieces together, *via* complexation, and the latter, the necessary chiral framework, frequently *via* a bidentate ligand auxiliary. Subtle steric effects,[4] arising from the interaction of the chiral pocket with the co-ordinated substrate, together with electronic effects,[5] induced by different donor atoms, can determine whether a given auxiliary will be successful for any one substrate.

2 Tactics

In both principle and practice, NMR spectroscopy offers unique opportunities for monitoring solution structures in chiral organometallics, and specifically, in the recognition of the subtle interplay between auxiliary and substrate.[6] However, since the proton spectra of mixtures of diastereomers containing, *e.g.*, complexed Binap [2,2′-bis(diphenylphosphino)-1,1′-binaphthyl], are often not readily amenable to interpretation, it is useful to have a plan of attack. In the last decade or so, we have advocated a simple 2-D NMR approach to confronting structural questions when the auxiliary is either a bidentate phosphine or contains a phosphorus donor. (1) Assign the ^{1}H resonances by correlating these to other spins, *e.g.* ^{31}P, ^{13}C, metals (such as ^{195}Pt or ^{103}Rh), or other protons. (2) Determine the solution 3-D structure, using ^{1}H NOE spectroscopy. (3) Check the flexibility of the chiral pocket *via* NOE (or ROE) results and (4) determine if and which exchange processes occur (phase sensitive NOESY or ROESY data). In addition to (1)–(4), there are always the usual empirical coupling constant and chemical shift correlations which function as supplementary aids.

The assignment is often the most tedious job, in that the chemist is, of necessity, immersed in the NMR details; nevertheless, the chemical return is well worth the time investment.

The following sections describe simple applications using the methods mentioned and relate, primarily, to structural problems of chiral complexes. Nevertheless, all of the examples illustrate a structural or dynamic subtlety. There are basically two NMR categories: one which uses coupling constants, *i.e.*, an 'X,H'-correlation, and one based on NOE-type measurements, which includes 2-D exchange spectroscopy. The latter is definitely the structural work-horse.

The chiral chelating ligands under discussion L^1–L^6, are shown in Scheme 1. Although the emphasis is primarily on the Pd–allyl complexes of L^1–L^6, the problems confronted are in many ways typical, and provide both aesthetically pleasing and practical examples of how these various NMR forms can help.

Paul Pregosin

Gerald Trabesinger

Professor Paul Pregosin was born in New York city in 1943 and received his Ph.D. degree from the City University of New York in 1970. Postdoctoral stays at Queen Mary College, London and the University of Delaware preceded his arrival at the ETH in Zurich in 1973, where he has remained ever since. His research interests include organometallic chemistry, homogeneous catalysis and NMR spectroscopy.

Dr. Gerald Trabesinger was born on the 9th October, 1968, in Balzers, Principality of Liechtenstein. After finishing the Gymnasium he spent four months in the chemical industry before starting his chemistry studies at the ETH/Zürich, in 1988. He received his diploma in February, 1994. His Ph.D. work, under the supervision of Professor P. S. Pregosin, was completed in 1997, and concerned structural and dynamic studies of organometallic catalysts. He is currently employed by the firm of SIKA in Zurich.

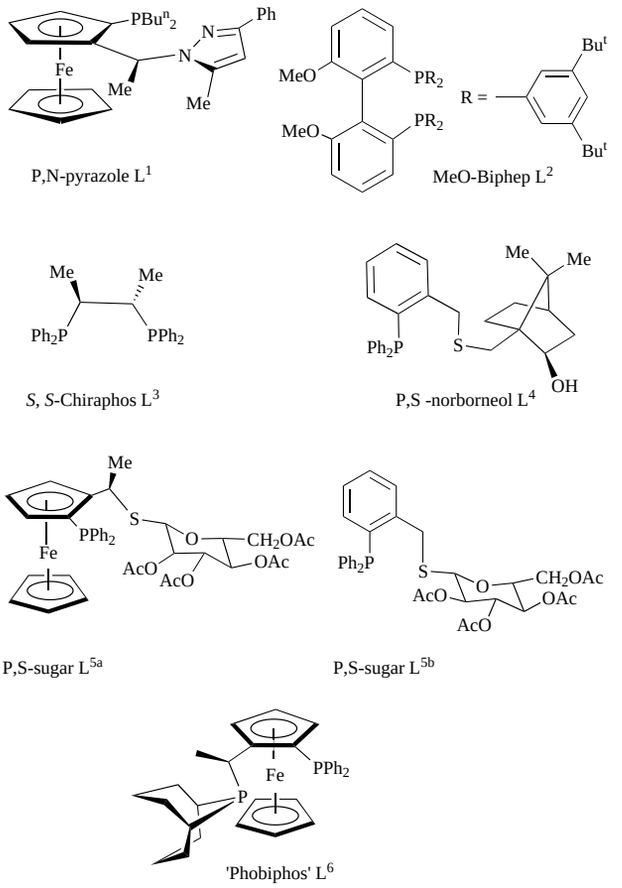

Scheme 1 Chiral chelating ligands

3 Correlations *via* Coupling Constants

^{31}P, ^{1}H Correlations

The Pd-catalysed enantioselective allylic alkylation reaction,[7] in which a new carbon–carbon bond is made [see equation (1)] has

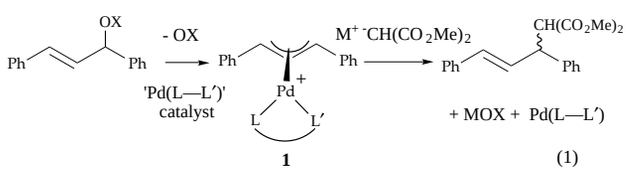

become quite popular. The test substrate is usually a 1,3-diphenylallyl acetate or carbonate of the type PhCH=CH–CH_2OX, X = *e.g.*, C(O)Me or CO_2Me. The cationic allyl intermediate **1** is often isolable[8,9] and has been the subject of considerable study.

An increasing number of chiral auxiliaries afford good-to-excellent enantiomeric excesses (e.e.s) for this particular transformation. Often P,N-chelating ligands[10–12] related to the phosphine–pyrazole chelate L^1 afford >95% e.e.s; however, the 1,3-diphenylallyl derivative $[Pd(\eta^3\text{-PhCHCHCHPh})(L^1)]^+$ **2**[13] is interesting for its complexity and not its effectiveness (*ca.* 20% e.e.). Complex **2** reveals four diastereomers in solution, A–D, in the ratio *ca.* 5 : 1.5 : 1 : 1. These might arise from (i) *syn*/*syn* or *syn*/*anti* structures or (ii) *exo*/*endo* isomers [the central allyl C–H bond can be pointing away from (*exo*) or towards (*endo*) the Fe atom] or (iii) chelate ring conformations which place the methyl group in either an equatorial or an axial position (see Scheme 2). It is always important to know which structural variations are accessible to any given auxiliary.

The structure proof starts by using a reliable empiricism: in allyl (and alkyl and olefin...*etc.*) complexes the value of $^3J(P,H)^{trans}$ is relatively large.[14] Consequently, a ^{31}P, ^{1}H correl-

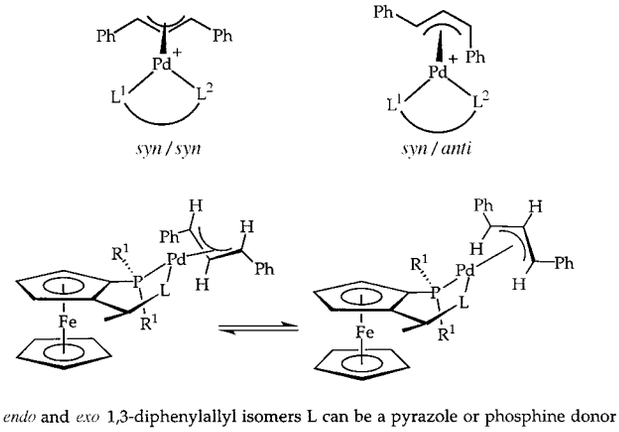

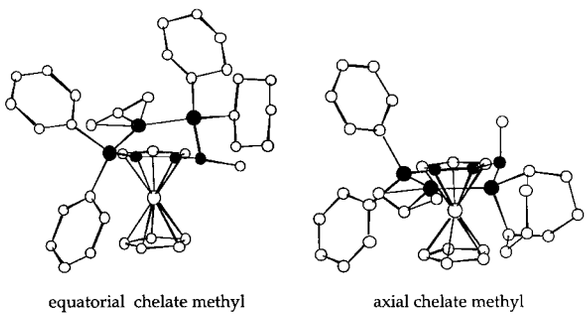

Scheme 2 Structural variations

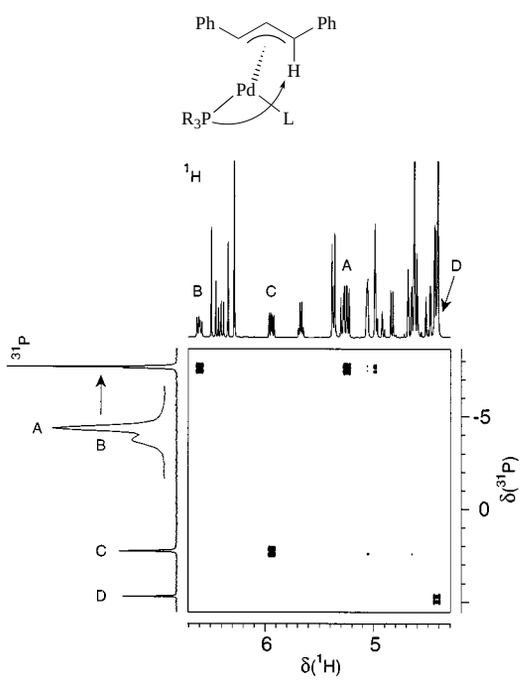

Fig. 1 ^{31}P, ^{1}H Correlation for $[Pd(\eta^3\text{-PhCHCHCHPh})(L^1)]PF_6$ **2** showing the four cross-peaks which arise from the allyl protons pseudo-*trans* to the P-donor

ation (see Fig. 1) can be used to select (assign) these terminal allyl signals. For **2**, the 2-D map shows the four cross-peaks which arise from these allyl resonances. Once these protons are assigned, inspection of NOE's from these resonances to the

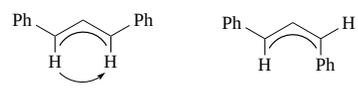

remaining allyl protons (see discussion of **12**, below) allows one to conclude that *all four isomers* have *syn*/*syn* structures, and,

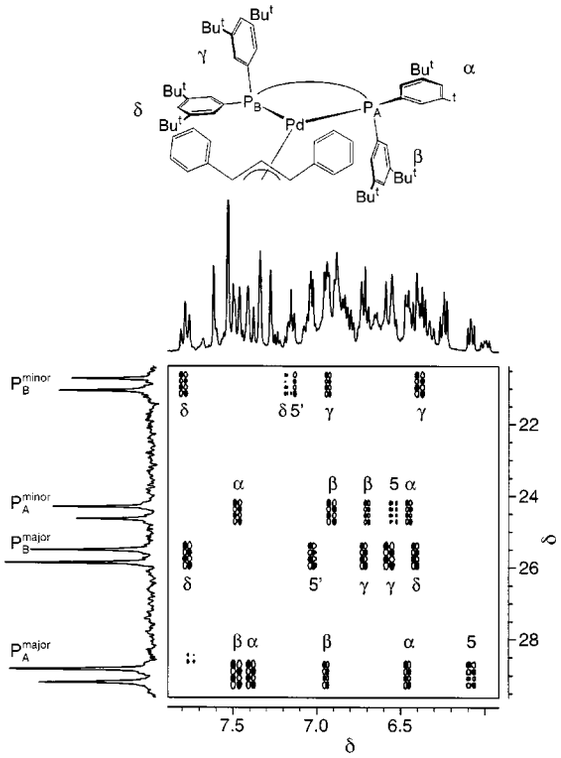

Fig. 2 ^{31}P, ^{1}H Correlation spectrum of the MeO-Biphep allyl complex **3**, showing the aromatic region. Five correlation peaks are visible for each ^{31}P-spin (20 for the two diastereomers): one each due to the biaryl protons, 5 and 5′ and *four* each from the non-equivalent phenyl *ortho* protons. Once these *ortho* protons are assigned, NOE results can be used for detailed structural work (CD_2Cl_2, 500 MHz, 193 K)

eventually, that the differing structures arise from points (ii) and (iii) (*exo* and *endo* plus two ring conformations). In **2** the phosphorus substituents do not intrude sufficiently into the allyl co-ordination sphere to induce isomerization to a *syn*/*anti* isomer.

Fig. 2 shows the ^{31}P, ^{1}H correlation for the MeO-Biphep derivative $[Pd(\eta^3\text{-PhCHCHCHPh})(L^2)]^+$ **3**.[15,16] The ^{31}P NMR spectrum shows that the complex exists in two forms. Using the logic above one can find the terminal allyl ^{1}H signals (not shown in Fig. 2) and show that, here, these *are* the *syn*/*syn* and *syn*/*anti* diastereomers.

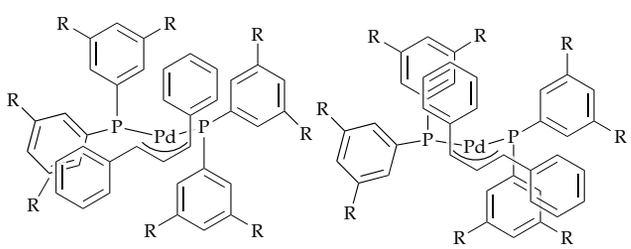

4 abbreviated *syn*/*anti* structures, R = Bu^t **5**
view from behind the allyl looking toward the auxiliary phenyl array

However, there are two possible *syn*/*anti* structures, abbreviated as **4** and **5**, which differ in terms of the allyl 'face' co-ordinated. To distinguish between these, we will need a detailed analysis of intraligand NOE's. Put differently, one needs to assign a series of 'reporter' protons,[17] so as to place the diphenylallyl ligand correctly, in 3-D space, relative to the auxiliary.

Here, the 'reporters' of choice are the *ortho* protons of the four P-aryl substituents, since these atoms are proximate to the co-ordinated allyl ligand. Assigning the aromatic region of the conventional 1-D proton spectrum may not look promising (see Fig. 2); however, the P,H-correlation uses the fairly large (5–10 Hz), ^3J(P,H) to select these *ortho* protons. As there are also two

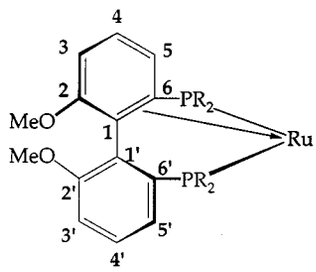

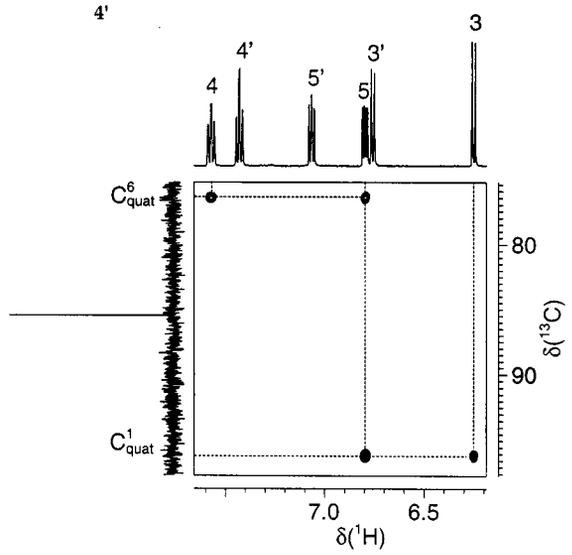

Fig. 3 Section of the long-range ^{13}C, ^{1}H correlation for **6**, R = Pr^i, showing the four key cross-peaks which link the resonances for the co-ordinated biaryl double bond to several of the biaryl proton resonances, *via* $^2J(^{13}C, ^{1}H)$ and, more importantly, $^3J(^{13}C, ^{1}H)$. The intense signal in the ^{13}C direction stems from one of the five $\eta^5\text{-}C_8H_{11}$ pentadienyl carbons (500 MHz, CD_2Cl_2, room temperature. Optimized for J = 8.3 Hz, since the values ^2J(C,H) and ^3J(C,H) are normally less than 10 Hz. Magnitude spectrum)

biaryl protons *ortho* to the P-donors (noted as 5 in Fig. 2), each ^{31}P resonance reveals *five* correlations [due to restricted rotation around the P–C(*ipso*) bonds]. With these signals recognised, one can use NOE's to assign **5** as correct (each terminal allyl proton in **5** is proximate to only *one* P-phenyl moiety, as opposed to two in **4**[18]).

The solution of simple structural problems such as those described for **2** and **3** represents a fundamental step in understanding steric interactions in co-ordinated chiral auxiliaries. Clearly, the P,H correlations start us down the right road.

^{13}C, ^{1}H Correlations

One usually knows how a given auxiliary co-ordinates; however, sometimes there are surprises. Fig. 3 reproduces part of the *long-range* C,H correlation from the MeO-Biphep cation $[Ru(\eta^5\text{-}C_8H_{11})(L^2)]^+$ **6** with R = Pr^i. Both the molecule and the

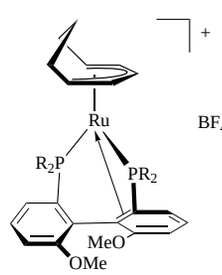

6

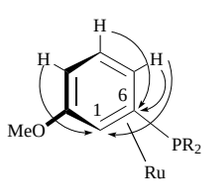

R = Pr^i or $C_6H_3Bu^t_2$-3,5
four correlations, two each to C^1 and C^6

7

spectrum require comment. In compound **6** one of the *biaryl* double bonds can co-ordinate to the Ru^{II} center, in addition to the P-donors.[19] This represents a rare bonding situation which was not recognised when the structure proof began.

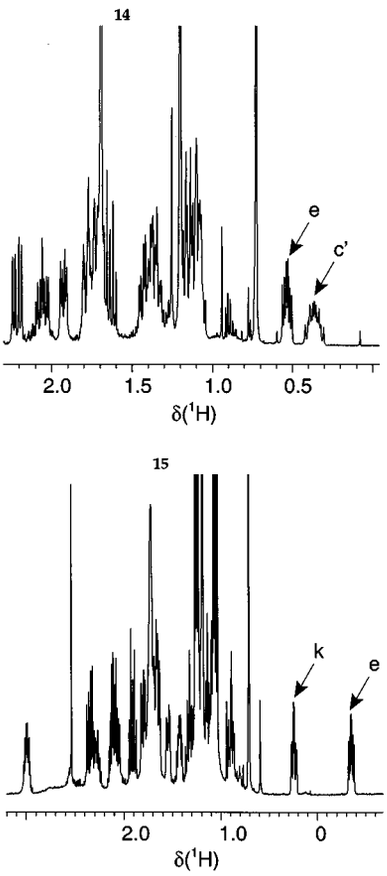

Fig. 4 Aliphatic regions of the ^{1}H spectra of the Binap and Chiraphos complexes **8** (top) and **9** (bottom), respectively, showing signals at unexpectedly low frequency. These shielded steroid protons (indicated by arrows) are due to the proximity of one of the P-phenyl rings of the auxiliary (CD_2Cl_2, 500 MHz, ambient temperature)

X-Ray crystallography[19] suggests rather long distances between the 1,6 double bond and the ruthenium. However, the ^{13}C NMR spectroscopy is clear, provided that *one knows how to find* the C^1 and C^6 signals! The 1-D carbon spectrum for **6**, shown as the ordinate of Fig. 3, is not revealing, due to long T_1's for C^1 and C^6 and multiplicity due to the ^{31}P spins. The only visible signal stems from one of the η^5-C_8H_{11} resonances. Nevertheless, there are four very clear cross-peaks in the 2-D map, which arise from the two- and three-bond couplings indicated in **7**. Since the intensity of these cross-peaks depends on both the proton and carbon magnetisations, there is no doubt as to the correct chemical shifts, δ 74.5 and 95.1, for C^6 and C^1, respectively, and these values are indicative of complexation.[20] It is not yet clear as to whether this co-ordination mode has any relevance to catalysis; however: (a) it certainly provides the complex with potential electronic flexibility, (b) the ligand class L^2 is very successful in enantioselective hydrogenation[16] and (c) it is now known[21,22] that Binap can also manage this type of interaction (see cover figure), so that this bonding may represent a general characteristic for biaryl-based ligands.

Occasionally, a carbon–proton correlation helps in clearing up a ^{1}H NMR ambiguity. Fig. 4 gives sections of the low frequency regions of the Binap and Chiraphos androstene allyl complexes **8** and **9**, respectively. From Fig. 4 it can be seen that there are several very low frequency resonances, and for the Chiraphos derivative **9** there is a signal at lower frequency than $SiMe_4$. A section of the C,H correlation for **9** is given in Fig. 5, and immediately reveals that both of these ^{1}H absorptions stem from methine carbons of a rather ordinary nature [based on the carbon positions and the measured ^1J(C,H) values]. The unexpected ^{1}H chemical shifts arise from the proximity of one of the P-phenyl substituents, *i.e.*, one is dealing with an anisotropic effect. This type of anisotropic effect is a common

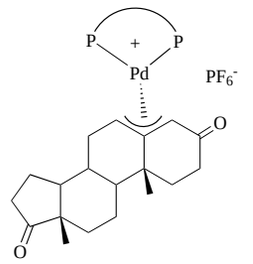

8 contains Binap and **9** contains *S*, *S*-Chiraphos

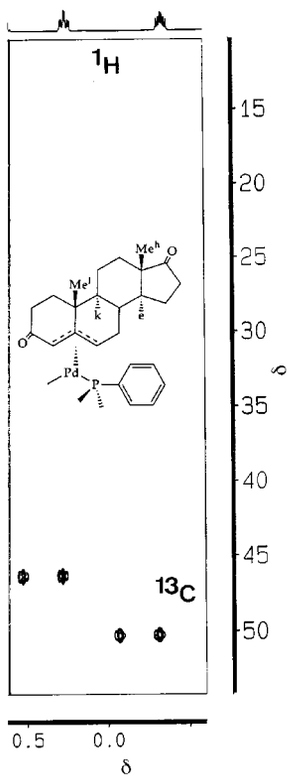

Fig. 5 Section of the ^{13}C, ^{1}H correlation for the Chiraphos complex **9** showing routine methine ^{13}C chemical shifts associated with the low frequency proton signals (CD_2Cl_2, 500 MHz, ambient temperature)

occurrence when dealing with relatively large 'intrusive' chiral P-phenyl auxiliaries.

^{195}Pt, ^{1}H Correlation

Metal–proton correlations in homogeneous catalysis[24,25] are useful, if somewhat rare. Moreover, the dichloro *exo*-norborneol P,S-complex $PtCl_2(L^4)$ **10** might seem out of place as it has no carbon ligand. Nevertheless, interest in **10** developed when the structures for $[M(\eta^3\text{-}C_3H_5)(L^4)]X$, M = Pd or Pt, X = CF_3SO_3 or PF_6 (as well as those for some Rh–COD complexes) could not be solved, due to the presence of four (or more) compounds, all dynamic on the NMR time-scale.[26] Further, the P,S-chelate L^4 is a rather poor auxiliary both in Rh-hydrogenation and Pd-alkylation chemistry. Initially, we considered the possibility that this thioether chelate does not complex strongly or perhaps its complexes undergo rapid sulfur-inversion (the S atom is a stereogenic centre[27]), with the result that the chiral pocket is too flexible. The dichloro-complex **10** allowed us to scrutinise some details of chelate co-ordination without the additional complexities associated with prochiral olefin or allyl ligands.

Despite its simplicity, **10** exists in solution in two forms which are in slow exchange on the NMR time-scale (*via* 2-D exchange spectroscopy).[26] Fig. 6, reproduces a section of the platinum–proton correlation for the key CH_2 protons, H^{11}_{eq} and H^{11}_{ax} with

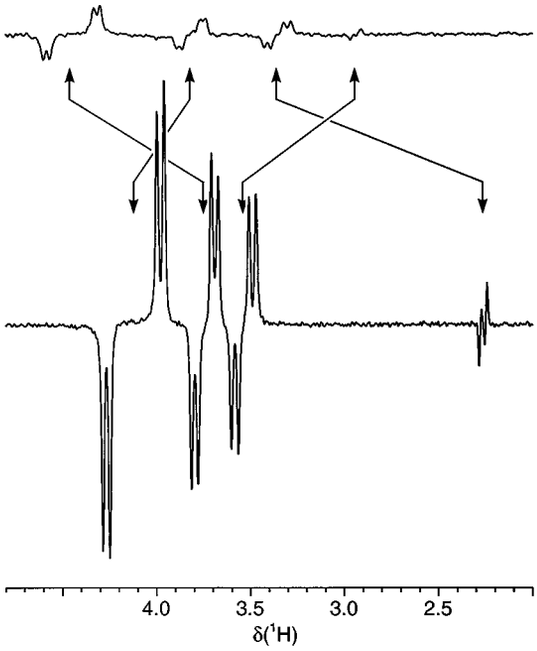

Fig. 6 ^{195}Pt Satellites from a section of the HMQC spectrum for the two isomers of $PtCl_2(L^4)$ **10**. The arrows indicate the exchange. Note that the highest frequency proton H^{11}_{eq}, with the relatively large ^3J coupling in the major isomer, is exchanging with proton H^{11}_{ax} with a much smaller ^3J coupling, in the minor isomer. In the lower trace, the first two anti-phase doublets come from H^{11}_{eq} and H^{11}_{ax}, and the second two anti-phase doublets stem from the norborneol S-CH_2, H^{10} δ ^{195}Pt (major) = −4166, δ ^{195}Pt (minor) = −4136 (400 MHz, $CDCl_3$)

the arrows indicating the exchange. The two isomers have different chemical shifts although the Pt scale is not given. Since this is a proton-detected double quantum spectrum,[1,28] all signals *not* coupled to the platinum are filtered, *i.e.*, one does not see the main bands, only the satellite signals. This makes the interpretation simpler even if the two Pt-satellites for any one signal have opposite phases.

Fragment **11** gives a view of the chelate ring. In keeping with

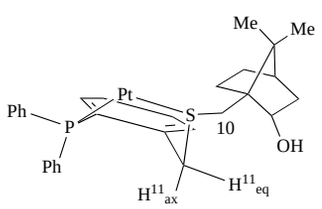

11

the Karplus relationship (which is also valid for ^{195}Pt[29]), one finds that the three-bond coupling ^3J(Pt,H) to the H^{11}_{eq} is larger than that for H^{11}_{ax}. Interestingly, from the 2-D exchange results, together with the different J values, one finds that H^{11}_{eq} in the major isomer is exchanging with H^{11}_{ax} in the minor isomer and, of course, H^{11}_{ax} in the major isomer with H^{11}_{eq} in the minor isomer. A chelate-ring inversion would account for these obser-

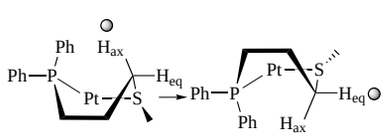

fragments of **11**; the grey ball shows H_{ax} before and after inversion

vations and also explain the poor enantioselectivity. The chiral environment, which resides on the sulfur substituent, is moving about, and thus prochiral organic substrates find little or nothing resembling a chiral pocket (Biphep and Binap-type

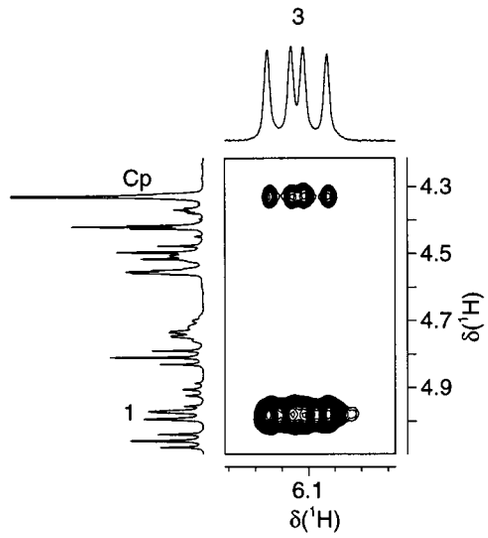

Fig. 7 Section of the ROESY spectrum for the P,S-sugar complex $[Pd(\eta^3\text{-PhCHCHCHPh})(L^5)]^+$ **12**, showing the strong H^1, H^3 intra-allyl NOE from the terminal protons (lower cross-peak) and the H^3 to η^5-Cp NOE; H^3 is pseudo-*trans* to phosphorus and spin–spin couples to one ^{31}P-spin and the central allyl proton (233 K, CD_2Cl_2, 500 MHz)

auxiliaries possess relatively rigid chiral pockets[30] and this, partly, explains their success). In the allyl complexes of L^4, the mixtures arise due to the ring conformations plus diastereomers from allyl (or in the Rh-chemistry, olefin) complexation. The platinum–proton correlation simplified the picture and the exchange results clarified the problem.

4 Overhauser and Exchange Spectroscopy

NOE studies

Once key protons are assigned, the way is clear for structural studies *via* NOE's Fig. 7 shows a section of the NOESY spectrum for the P,S-sugar complex, $[Pd(\eta^3\text{-PhCHCHCHPh})(L^{5a})]^+$ **12**[31] and presents a repetition of our standard approach

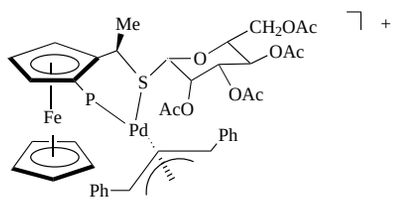

12

to assigning *syn*/*syn vs*. *syn*/*anti* structures. All allyl *syn*/*syn* structures show modest-to-strong NOE's between the two *anti* protons, as indicated by the lower cross-peak in Fig. 7. Since *anti* allyl protons (but not the *syn* protons) bend selectively *out of the allyl plane*, away from the metal,[17,32] complete reliance on

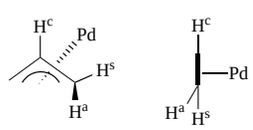

two views of of a Pd–allyl showing the selective *anti* distortion: left, from behind the allyl, right from the side (H^c = central proton)

^3J(H,H) as a structure probe, with its associated dihedral angle dependence, is not always safe. Fig. 7 also shows a weaker cross-peak from an *anti* allyl proton to the η^5-Cp, of the ferrocene, a rare example of using this Cp-signal to determine whether the allyl is *exo* or *endo* with respect to the auxiliary. This latter NOE most likely arises due to rotation of the allyl ligand,[31] relative to

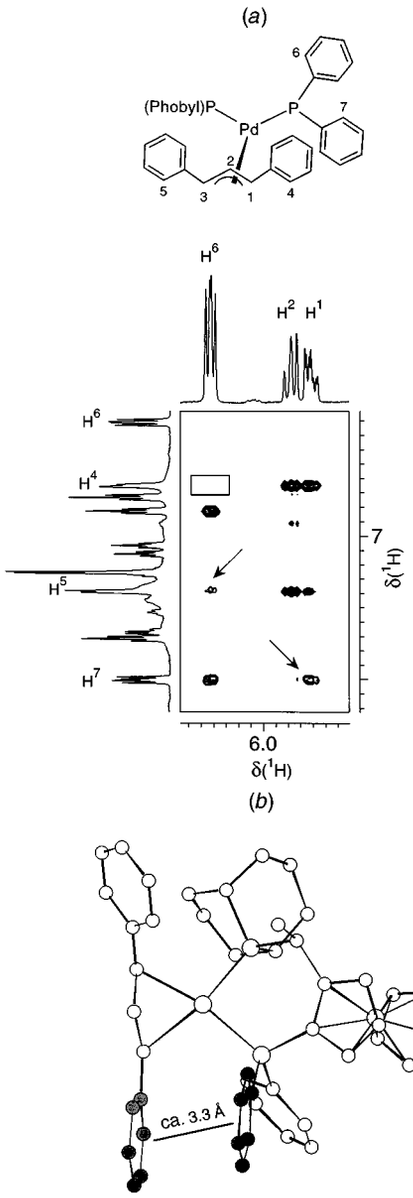

Fig. 8 (*a*) Section of the phase-sensitive NOESY spectrum of the cation $[Pd(\eta^3\text{-PhCHCHCHPh})(L^6)]^+$ **13**, which suggests that the two rings with H^4 and H^6 as *ortho*-protons are stacked. The rectangle indicates where one would expect a cross-peak if there were no synchronous rotation. The H^5, H^6 cross-peak indicated by an arrow arises from allyl rotation. The H^1, H^7 cross-peak stems from the pseudo-axial position of the ring containing H^7. (*b*) MoMo view of the 'Phobiphos' cation $[Pd(\eta^3\text{-PhCHCHCHPh})(L^6)]^+$ **13**, based on X-ray crystallography, showing the stacking of two phenyl groups

the P–Pd–S plane, thus bringing one *anti* proton closer to the η^5-Cp.

Fig. 8(*a*) shows a section of the NOESY spectrum for the 'phobiphos' cation [33] $[Pd(\eta^3\text{-PhCHCHCHPh})(L^6)]^+$ **13** abbreviated above, and represents a case where the absence of an NOE is structurally significant. When phenyl groups from both the auxiliary and the substrate come close in space they may

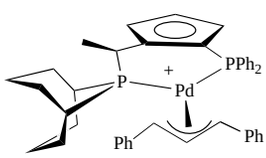

13 (Fe and lower Cp omitted for clarity)

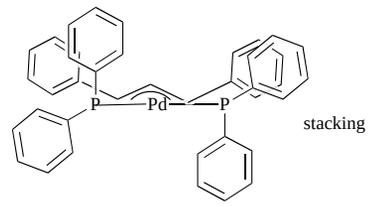

fragment of a 1,3-diphenylallyl Pd complex showing, in this case, an *S*-type Biphep chiral pocket and stacking

'stack'.[33] The pseudo-equatorial rings containing H^4 and H^6, shown in Fig. 8(*a*), need not lie perfectly over one another, however, the stacking is such that the rings rotate synchronously at ambient temperature. Although the substituents are only *ca.* 3.3–3.4 Å apart,[32] as shown in Fig. 8(*b*), the synchronous rotation prevents the development of significant NOE's between the two (H,H contacts of *ca.* 3 Å or less are required). Thus, the missing cross-peaks [the empty rectangle in Fig. 8(*a*)] are typical and suggest this type of stacking. The NOE's between the *ortho* protons H^6 and H^7, as well as between the allyl H^1 and *ortho* H^7, are readily observed. This stacking is a structural compromise and, for **13**, analysis of the allyl ^{13}C chemical shift data suggests that this interaction is repulsive. In chiral 1,3-diphenylallyl complexes of Pd^{II}, stacking is fairly common.

Exchange spectra

In a routine NOESY spectrum, the phases of the NOE cross-peaks are usually opposite to those of the diagonal. However, when chemical exchange takes place, the exchange cross-peaks appear with the same phase as the diagonal,[34] thus providing an often unexpected bonus.

For this author, exchange (NOE) spectroscopy is most gratifying when it reveals one or more compounds whose presence would normally have gone unnoticed. This is the case for the P,S-sugar Pd^0 complex $[PdR(L^{5b})]$ **14** (R = benzoquinone).[35]

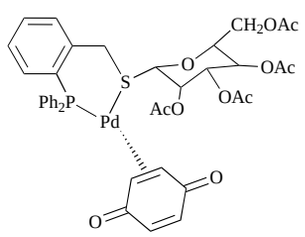

14

Chiral zero-valent complexes are often postulated as intermediates in a variety of Pd-catalysed reactions, *e.g.*, the enantioselective Heck reaction, but few of these compounds have been isolated.[35–38]

As shown in Fig. 9, the three-co-ordinate complex **14** shows four well resolved olefinic signals from the quinone: two at *ca.* δ 6.0, H^5 and H^6, plus two from the complexed double bond, close to δ 5.2, H^2 and H^3. Complex **14** might exchange the two double bonds of the benzoquinone *via* an intramolecular process as suggested by equation (2). However, the exchange

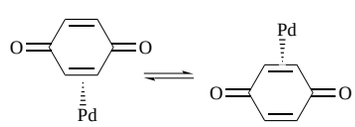

(2)

spectrum shows that this is not correct. Although there are strong cross-peaks which indicate the random exchange of all four protons, there are also exchange cross-peaks from all four protons to an 'invisible' signal between δ 6.7 and 6.8, the position of uncomplexed benzoquinone. Although the free

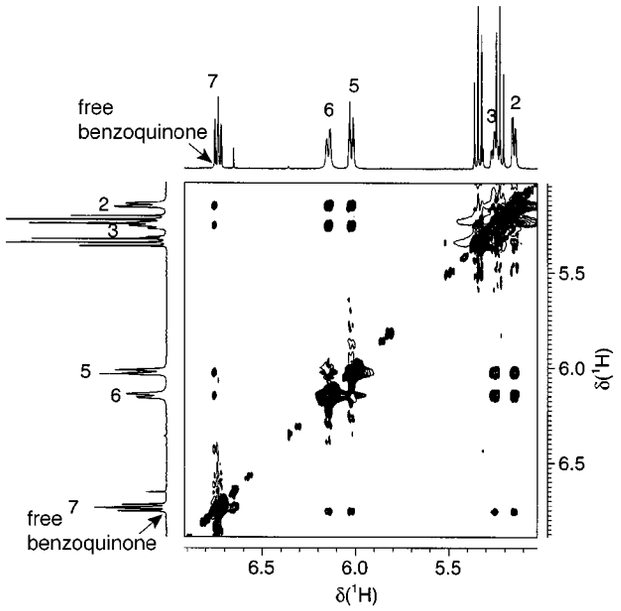

Fig. 9 Section of the phase-sensitive NOESY spectrum of the P,S-sugar Pd^0 benzoquinone complex **14** revealing the random exchange of the four olefinic protons H^2,H^3 and H^5,H^6, from the complexed benzoquinone with the free ligand (500 MHz, CD_2Cl_2)

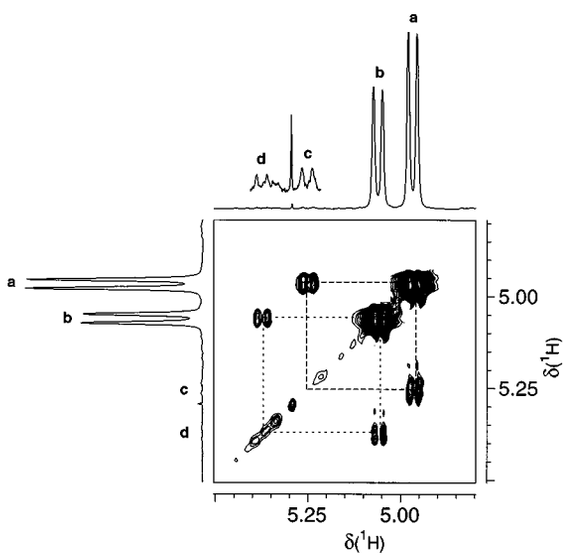

Fig. 10 Section of the phase-sensitive NOESY spectrum of the P,S-*exo*-norborneol complex [Pd(η^3-PhCHCHCHPh)(L^4)]$^+$ **15**,[39] revealing the selective exchange between the ally protons of the four isomers. Isomers a and b are assigned allyl *syn*/*syn* structures with *exo* and *endo* configurations. Isomers c and d are assigned *syn*/*anti* structures with *exo* and *endo* configurations. Note that c and d are not readily detected in the 1-D spectrum. The protons shown are pseudo-*trans* to sulfur. The sharp ^{1}H signal between c and d stems from a trace of CH_2Cl_2 ($CDCl_3$, 296 K)

quinone is only present in traces, the cross-peaks reveal the exchange to be intermolecular in nature.

In enantioselective catalysis one is often concerned with small quantities of diastereomers which might be kinetically important. Fig. 10 presents a section of the exchange spectrum for the cationic *exo*-norborneol complex [Pd(η^3-PhCHCHCHPh)(L^4)]$^+$ **15**,[39] and shows only the region of the allyl-proton pseudo-*trans* to the sulfur donor. At first glance it would appear that there are only two species, **a** and **b**, which are not in exchange; however, there are clearly two more complexes, **c** and **d** which are essentially invisible in the 1-D spectrum, but which are involved in a selective exchange with **a** and **b**. It can be shown that the exchange develops from the usual η^3-η^1-η^3-isomerization reaction.[40–45] Nevertheless, neither the existence

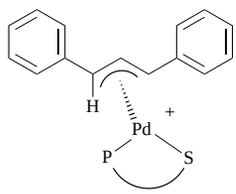

of **c** and **d** nor their dynamics were obvious before the exchange spectroscopy. Figs. 10 and 11 provide nice examples of how exchange spectroscopy provides mechanistic insights.

In terms of chiral catalysis, there are more relevant examples of the importance of exchange spectroscopy. In the allylic alkylation of equation (1), the (*S*)-MeO-Biphep L^2 affords the (+) enantiomer in *ca*. 91% e.e.[15] However, as noted above, **3**, the presumed intermediate, exists as two diastereomers with similar populations. Since the nucleophile can attack four different allyl termini, there must be a specific selection process to account for the observed e.e. One explanation which unites these observations invokes an equilibrium in solution such that a 'pump' exists (*i.e.*, the Curtin–Hammett principle is valid as suggested early on by Bosnich[46]). In fact, the same phase-sensitive NOE spectrum which distinguished between **4** and **5**, clearly revealed positive-phase cross-peaks indicating an equilibrium between the structural types **16** and **17**. Using exchange spectroscopy one can show equilibria, not only for **3**, but for the allyl compounds **2**, **13** and [Pd(η^3-PhCHCHCHPh)(Binap)]$^+$ **18**, amongst others, although the interconversions may take different forms, *e.g.*, *exo*-to-*endo* instead of *syn*/*syn*-to-*syn*/*anti*. The populations of the observed allyl intermediates in an enantioselective allylic alkylation reaction need not (but can) reflect an observed e.e.

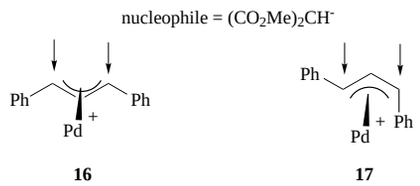

16 **17**

arrows indicate possible sites of the nucleophilic attack

5 Conclusion

The complexes and spectra presented above touched on problems concerned with geometric isomers (**2**), prochiral face selection (**3**), a new bonding mode for Biphep (**7**), anisotropic effects (**8**, **9**), chelate ring inversion (**10**), phenyl stacking (**13**), detecting small quantities of exchanging species (**14**, **15**) and equilibrating diastereomers (**3**, **13**, **18**). The NMR solutions offered are not unique, but have the advantage of being somewhat broader than other classical approaches, *e.g.*, the same NOE spectrum that assigned structure, produced exchange information; the same ^{13}C spectrum that established a new bonding mode helped to identify the η^5-C_8H_{11} of **6** (a point which was glossed over); the ^{31}P, ^{1}H and ^{195}Pt, ^{1}H correlations assigned, filtered, and simplified, simultaneously...*etc*. When taken together, as they were in the examples, these methods represent a potent approach to the problems of structure and dynamics in chiral complexes.

6 Acknowledgements

P. S. P. thanks the Swiss National Science Foundation, the ETH Zurich and F. Hoffmann-La Roche AG, Basel, for financial support as well as Johnson Matthey for the loan of precious metals. Special thanks are also due to Professors A. Togni and A. Albinati for fruitful collaborative efforts over many years.

7 References

1 *Advanced Applications of NMR to Organometallic Chemistry*, eds. M. Gielen, R. Willem and B. Wrackmeyer, John Wiley and Sons, Chichester, 1996; H. Kessler, M. Gehrke and C. Griesinger, *Angew. Chem., Int. Ed. Engl.*, 1988, **27**, 490.

2 M. Billeter, Y. Q. Qian, G. Otting, M. Mueller, W. Gehring and K. Wuethrich, *J. Biol. Chem.*, 1993, **234**, 1084.

3 B. M. Trost and R. I. Higuchi, *J. Am. Chem. Soc.*, 1996, **118**, 10 094; B. M. Trost and Y. Li, *J. Am. Chem. Soc.*, 1996, **118**, 6625.

4 A. Pfaltz, *Acta Chim. Scand.*, 1996, **50**, 189; *Acc. Chem. Res.*, 1993, **26**, 339.

5 O. Loiseleur von Matt, G. Koch, A. Pfaltz, C. Lefeber, T. Feucht and G. Helmchen, *Tetrahedron: Asymmetry*, 1994, **5**, 573.

6 H. Rüegger, R. W. Kunz, C. J. Ammann and P. S. Pregosin, *Magn. Reson. Chem.*, 1992, **29**, 197; P. von Matt, G. C. Lloyd-Jones, A. B. E. Minidis, A. Pfaltz, L. Macko, M. Neuburger, M. Zehnder, H. Rüegger and P. S. Pregosin, *Helv. Chim. Acta*, 1995, **78**, 265.

7 B. M. Trost and D. L. van Vranken, *Chem. Rev.*, 1996, **96**, 395; T. Hayashi, M. Yamane and A. Ohno, *J. Org. Chem.*, 1997, **62**, 204; T. Hayashi, in *Catalytic Asymmetric Synthesis*, ed. I. Ojima, VCH Publishers, Weinheim, 1993, p. 325; O. Reiser, *Angew. Chem.*, 1993, **105**, 576.

8 A. Togni, U. Burckhardt, V. Gramlich, P. Pregosin and R. Salzmann, *J. Am. Chem. Soc.*, 1996, **118**, 1031; T. Hayashi, A. Yamamoto, Y. Ito, E. Nishioka, H. Miura and K. Yanagi, *J. Am. Chem. Soc.*, 1989, **111**, 6301.

9 J. Sprinz, M. Keifer, G. Helmchen, M. Reggelein, G. Huttner and L. Zsolnai, *Tetrahedron Lett.*, 1994, **35**, 1523; M. Moreno-Manas, F. Pajuela, T. Parella and R. Pleixats, *Organometallics*, 1997, **16**, 205; M. Prat, J. Ribas and M. Moreno-Manus, *Tetrahedron*, 1992, **48**, 1695.

10 U. Burckhardt, L. Hintermann, A. Schnyder and A. Togni, *Organometallics*, 1995, **14**, 5415; P. Blochl and A. Togni, *Organometallics*, 1996, **15**, 4125; T. Ward, *Organometallics*, 1996, **15**, 2836.

11 J. M. Valk, T. D. W. Claridge, J. M. Brown, D. Hibbs and M. B. Hursthouse, *Tetrahedron: Asymmetry*, 1995, **6**, 2597; J. M. Brown, D. I. Hulmes and P. J. Guiry, *Tetrahedron*, 1994, **50**, 4493.

12 H. Rieck and G. Helmchen, *Angew. Chem.*, 1995, **107**, 2881; J. M. Williams, *Synlett*, 1996, 705.

13 R. Salzmann, Ph.D. Thesis no. 11443, ETHZ, 1996. We thank Professor A. Togni for the complex.

14 P. S. Pregosin and R. W. Kunz, in *NMR Basic Principles and Progress*, eds. P. Diehl, E. Fluck and R. Kosfeld, Springer Verlag, Berlin, 1979, p. 28.

15 G. Trabesinger, A. Albinati, N. Feiken, R. W. Kunz, P. S. Pregosin and M. Tschoerner, *J. Am. Chem. Soc.*, 1997, **119**, 6315.

16 For the preparation and additional chemistry of Biphep ligands see: Y. Crameri, J. Foricher, U. Hengartner, C. Jenny, F. Kienzle, H. Ramuz, M. Scalone, M. Schlageter, R. Schmid and S. Wang, *Chimica*, 1997, **51**, 303; R. Schmid, E. A. Broger, M. Cereghetti, Y. Crameri, J. Foricher, M. Lalonde, R. K. Mueller, M. Scalone, G. Schoettel and U. Zutter, *Pure Appl. Chem.*, 1996, **68**, 131; B. Heiser, E. A. Broger and Y. Crameri, *Tetrahedron: Asymmetry*, 1991, **2**, 51 and refs. therein.

17 A. Albinati, R. W. Kunz, C. Ammann and P. S. Pregosin, *Organometallics*, 1991, **10**, 1800; 1990, **9**, 1826.

18 P. S. Pregosin and R. Salzmann, *Magn. Reson. Chem.*, 1994, **32**, 128; P. S. Pregosin, H. Rüegger, R. Salzmann, A. Albinati, F. Lianza and R. W. Kunz, *Organometallics*, 1994, **13**, 5040.

19 N. Feiken, P. S. Pregosin and G. Trabesinger, *Organometallics*, 1997, **16**, 537.

20 B. E. Mann and B. F. Taylor, *^{13}C NMR Data for Organometallic Compounds*, Academic Press, London, 1981, p. 254; M. A. Bennett, I. J. McMahon, S. Pelling, M. Brookhart and D. M. Lincoln, *Organometallics*, 1992, **11**, 127.

21 D. D. Pathak, H. Adams, N. A. Bailey, P. J. King and C. White, *J. Organomet. Chem.*, 1994, **479**, 237.

22 N. Feiken, P. S. Pregosin and G. Trabesinger, *Organometallics*, 1998, **16**, 5756.

23 D. Drommi, R. Nesper, P. S. Pregosin, G. Trabesinger and F. Zürcher, *Organometallics*, 1997, **16**, 4268.

24 ^{103}Rh is potentially useful. See, V. Tedesco and W. von Philipsborn, *Organometallics*, 1995, **14**, 3600; B. R. Bender, M. Koller, D. Nanz and W. von Philipsborn, *J. Am. Chem. Soc.*, 1993, **115**, 5889; J. M. Ernsting, C. J. Elsevier, W. D. J. de Lange and K. Timmer, *Magn. Reson. Chem.*, 1991, **29**, S 118; D. H. Imhof, H. Rüegger, L. M. Venanzi and T. R. Ward, *Magn. Reson. Chem.*, 1991, **29**, 73.

25 P. S. Pregosin, in *Encyclopedia of Nuclear Magnetic Resonance*, John Wiley and Sons, London, 1996, vol. 4, p. 2549.

26 A. Albinati, J. Eckert, P. S. Pregosin, H. Rüegger, R. Salzmann and C. Stoessel, *Organometallics*, 1997, **16**, 579.

27 E. Abel, D. G. Evans, J. R. Koe, V. Sik, M. B. Hursthouse and P. A. Bates, *J. Chem. Soc., Dalton Trans.*, 1989, 2315; E. Abel, J. C. Domer, D. Ellis, K. G. Orrell, V. Sik, M. B. Hursthouse and M. H. Mazid, *J. Chem. Soc., Dalton Trans.*, 1992, 1073.

28 R. Benn and A. Rufinska, *Magn. Reson. Chem.*, 1988, **26**, 895; R. Benn and C. Brevard, *J. Am. Chem. Soc.*, 1986, **108**, 5622; D. Nanz and W. von Philipsborn, *J. Magn. Res.*, 1991, **92**, 560.

29 L. E. Erickson, J. E. Sarneski and C. N. Reilley, *Inorg. Chem.*, 1975, **14**, 3007; 1978, **17**, 1701; S. Yano, T. Tukada and S. Yoshikawa, *Inorg. Chem.*, 1978, **17**, 2520 and refs. therein for Karplus-type relationships involving ^{195}Pt with ^{13}C and ^{1}H.

30 P. Barbaro, P. S. Pregosin, R. Salzmann, A. Albinati and R. W. Kunz, *Organometallics*, 1995, **14**, 5160.

31 A. Albinati, P. S. Pregosin and K. Wick, *Organometallics*, 1996, **15**, 2419.

32 R. Goddardd, C. Krüger, F. Mark, R. Stansfield and X. Zhang, *Organometallics*, 1985, **4**, 285; J. W. Faller, C. Blankenship and B. Whitmore, *Inorg. Chem.*, 1985, **24**, 4483; J. E. Gozum, D. M. Pollina, J. Jensen and G. S. Girolami, *J. Am. Chem. Soc.*, 1988, **110**, 2688; T. Clark, C. Rohde and P. von Rague Schleyer, *Organometallics*, 1983, **2**, 1344.

33 H. C. L. Abbenhuis, U. Burckhardt, V. Gramlich, C. Koellner, P. S. Pregosin, R. Salzmann and A. Togni, *Organometallics*, 1995, **14**, 759.

34 W. E. Hull, in *Two-Dimensional NMR Spectroscopy. Applications for Chemists and Biochemists*, VCH, New York, 1987, p. 153; R. R. Ernst, *Chimia*, 1987, **41**, 323.

35 M. Tschoerner, G. Trabesinger, A. Albinati and P. S. Pregosin, *Organometallics*, 1997, **16**, 3447.

36 H. Steinhagen, M. Reggelin and G. Helmchen, *Angew. Chem.*, 1997, **109**, 2199.

37 W. A. Herrmann, W. Thiel, C. Broßmer, K. Oefele and T. Priermeiler, *J. Organomet. Chem.*, 1993, **461**, 51; R. Fernandez-Galan, F. A. Jalon, B. R. Manzano, J. Rodriguez-de la Fuente, M. Vrahami, B. Jedlicka, W. Weissensteiner and G. Jogl, *Organometallics*, 1997, **16**, 3758.

38 C. Bolm, D. Kaufmann, S. Gessler and K. Harms, *J. Organomet. Chem.*, 1995, **502**, 47.

39 J. Herrmann, P. S. Pregosin, R. Salzmann and A. Albinati, *Organometallics*, 1995, **14**, 3311.

40 P. S. Pregosin and R. Salzmann, *Coord. Chem. Rev.*, 1996, **155**, 35.

41 J. W. Faller, *Determination of Organic Structures by Physical Methods*, eds. F. C. Nachod and J. J. Zuckerman, Academic Press, New York, 1973, vol. 5, p. 75; J. Faller and M. E. Thomsen, *J. Am. Chem. Soc.*, 1969, **91**, 6871; J. Faller, M. J. Incorvia and M. E. Thomsen, *J. Am. Chem. Soc.*, 1969, **91**, 518.

42 E. Cesarotti, M. Grassi, L. Prati and F. Demartin, *J. Chem. Soc., Dalton Trans.*, 1991, 2073; *J. Organomet. Chem.*, 1989, **370**, 407.

43 A. Gogoll, J. Ornebro, H. Grennberg and J. E. Bäckvall, *J. Am. Chem. Soc.*, 1994, **116**, 3631.

44 H. Kurosawa, K. Shiba, K. Hirako, K. Kakiuchi and I. Ikeda, *J. Chem. Soc., Chem. Commun.*, 1994, 1099.

45 B. Crociani, F. Di Bianca, L. Canovese and P. Uguagliati, *J. Organomet. Chem.*, 1990, **381**, C17; B. Crociani, F. Di Bianca, L. Canovese, P. Uguagliati and A. Berton, *J. Chem. Soc., Dalton Trans.*, 1991, 71.

46 P. B. Mackenzie, J. Whelan and B. Bosnich, *J. Am. Chem. Soc.*, 1985, **107**, 2046; P. R. Auburn, P. B. Mackenzie and B. Bosnich, *J. Am. Chem. Soc.*, 1985, **107**, 2033.

Received 27*th November* 1997; *Paper* 7/08568K